View Online / Journal Homepage / Table of Contents for this issue
Dynamic Article Links

Soft Matter

Cite this: *Soft Matter*, 2011, **7**, 3219

www.rsc;org/softmatter

PAPER

Hydrodynamic interactions enhance the performance of Brownian ratchets

Andrej Grimm[a] **and Holger Stark***[b]

Received 1st October 2010, Accepted 6th December 2010
DOI: 10.1039/c0sm01085e

Published on 24 December 2010 on http://pubs.rsc.org | doi:10.1039/C0SM01085E
Downloaded by TU Berlin - Universitaetsbibl on 23 March 2012

We investigate how hydrodynamic interactions between Brownian particles influence the performance of a fluctuating ratchet. For this purpose, we perform Brownian dynamics simulations of particles that move in a toroidal trap under the influence of a sawtooth potential which fluctuates between two states (on and off). Hydrodynamic interactions are included in the Rotne-Prager approximation. We first consider spatially constant transition rates between the two ratchet states and observe that hydrodynamic interactions significantly increase the mean velocity of the particles but only when they are allowed to change their ratchet states individually. If in addition the transition rate to the off state is localized at the minimum of the ratchet potential, particles form characteristic transient clusters that travel with remarkably high velocities. The clusters form since drifting particles have the ability to push but also pull neighboring particles due to hydrodynamic interactions.

1. Introduction

Hydrodynamic interactions are ubiquitous in colloidal systems, as particles moving in a viscous fluid induce a flow field that effects other particles in their motion.[1–3] Early experimental and theoretical studies mostly investigated macroscopic rheological or transport properties of colloidal suspensions, where hydrodynamic interactions only appear in ensemble averages over the complete configuration space.[4,5] Recent advances in experimental techniques such as video microscopy and optical tweezers[6] have made it possible to monitor and manipulate single particles. This also includes various realizations of a Brownian ratchet.[7–11] In this article we study how hydrodynamic interactions between several colloidal particles influence the performance of a fluctuating Brownian ratchet.[12–14]

In order to systematically investigate the role of hydrodynamic coupling, studies were performed on the diffusion of an isolated pair of particles or the correlated thermal fluctuations of two colloidal beads held at a fixed distance by an optical tweezer.[15–18] Several interesting collective phenomena were identified that originate from the long-range nature of hydrodynamic interactions. For instance, they give rise to periodic or almost periodic motions or even transient chaotic dynamics in sedimenting clusters of a few spherical particles.[19–21] Hydrodynamic interactions also lead to pattern formation through self-assembly of rotating colloidal motors or in arrays of microfluidic rotors.[22–24] Synchronization induced by hydrodynamic interactions is particularly important in microbiology. Metachronal waves occur in arrays of short filaments that cover, for example, a paramecium. In order to shed light on the origin of these waves, synchronization in model systems consisting of a few particles was studied.[25–29] Rotating helices such as bacterial flagella but also Eukaryotic flagella synchronize through hydrodynamic interactions,[30–32] and even microscopic swimmers are hydrodynamically coupled.[33–35]

The theoretical study presented in this article is based on a toroidal trap set-up that has proven to be useful for investigating in detail hydrodynamic interactions among a limited number of particles.[36,37] The toroidal trap is realized by means of a circling optical-tweezer focus that forces particles to move along a circle. For a cluster of particles, each driven by a constant force, theory has demonstrated highly non-linear drafting behavior[36] which was then observed in experiments.[37] Modulating the laser intensity during one cycle, one can apply additional tangential driving forces to the particles so that a tilted sawtooth potential results. Here, hydrodynamic interactions help the particles to leave the local minima of the potential and thereby create caterpillar-like motion patterns. As a result, the particle cluster moves with a significantly increased mean velocity compared to a single particle in the same potential.[37]

How hydrodynamic interactions influence the performance of ratchet systems has so far been investigated in two numerical studies. In the first study, hydrodynamic coupling was included in the asymmetric simple exclusion process (ASEP) as a model for the dynamics of Brownian motors.[38] In the second study, hydrodynamic interactions were taken into account in Brownian dynamics simulations of a harmonically coupled dimer in a ratchet potential.[39] Both studies reported increased mean velocities of the Brownian motors and dimers, respectively, due to hydrodynamic coupling. However, the mechanism causing the enhanced velocities has not been studied in detail.

[a]*National University of Singapore, Department of Physics, 2 Science Drive 3, 117542, Singapore*
[b]*Institut für Theoretische Physik, Technische Universität Berlin, Hardenbergstrasse 36, D-10623 Berlin, Germany. E-mail: holger.stark@tu-berlin.de*

View Online

Published on 24 December 2010 on http://pubs.rsc.org | doi:10.1039/C0SM01085E
Downloaded by TU Berlin - Universitaetsbibl on 23 March 2012

In this article, we investigate how pure hydrodynamic coupling influences the collective dynamics of colloidal particles in a fluctuating ratchet potential within a toroidal trap. We use the Rotne-Prager approximation to include hydrodynamic interactions into our Brownian dynamics simulations. Of particular interest is the rate with which the ratchet potential is switched off. We begin with a spatially constant rate along the toroidal trap and demonstrate that hydrodynamic interactions increase the mean particle velocity only when colloids are able to change their ratchet states individually. We then allow for transition rates localized around the potential minima and show how hydrodynamic interactions induce the formation of long-lived transient clusters that travel along the toroidal trap with velocities an order of magnitude larger than a single particle. The ability of particles to pull their neighbors due to hydrodynamic interactions is essential for the observed cluster formation.

The article is organized as follows. In Section 2, we introduce the toroidal trap as our model system and the applied ratchet potential. Then hydrodynamic interactions and their implementation within the Langevin equation are explained. The section ends with details of the Brownian dynamics simulations and of our observables, the mean particle velocity and the velocity auto-correlation function. Section 3.1 summarizes the results for the single-particle system as it serves as a reference for the multi-particle systems treated thereafter. In Section 3.2, we first discuss how hydrodynamic interactions influence the performance of the ratchet when the transition rates between the ratchet states do not depend on the particle positions. Two operational modes are studied: in the first mode, all particles change their ratchet state simultaneously while in the second mode they change it individually. Finally, in Section 3.3 we introduce localized transition rates and demonstrate how hydrodynamic interactions induce the formation of transient clusters. The article ends with concluding remarks.

2. Model and numerical implementation

We choose a toroidal trap as a model system since such a system has already been used for related numerical studies of hydrodynamic phenomena in colloidal systems and has been realized experimentally.[36,37]

2.1. Toroidal trap

The toroidal trap contains N spherical particles with radius σ. Their positions are specified by cylindrical coordinates (r,ϕ,z) and $\boldsymbol{r}$ is the positional vector. A harmonic trap potential V_{trap} of the form

$$V_{\mathrm{trap}} = \frac{A}{2}\left[(r-R)^2+z^2\right] \tag{1}$$

keeps the particles on a circle with radius R. In the following, we chose A such that the particles are not able to change their sequential order.

The interaction between the particles is modeled with a soft repulsive potential V_{rep} of the form

$$V_{\mathrm{rep}} = B\left[\left(\frac{r_{ij}}{2\sigma}\right)^{12}-1\right]^{-1}. \tag{2}$$

Here, $r_{ij}=|\boldsymbol{r}_i-\boldsymbol{r}_j|$ is the center-center distance between particles i and j. In the following, we chose B such that the minimal distance during the simulations is approximately 3σ.

2.2. Ratchet potential and transition rates

A sawtooth-type ratchet potential $V_{\mathrm{rat}}(\phi)$ is imposed in tangential direction. As illustrated in Fig. 1, the ratchet potential is characterized by the angular period L_ϕ, the asymmetry parameter a, and the amplitude $\hat{V}_{\mathrm{rat}}$ through

$$V_{\mathrm{rat}}(\phi) = \hat{V}_{\mathrm{rat}}\begin{cases} \dfrac{\phi}{aL_\phi} & \text{for } 0<aL_\phi, \\ 1-\dfrac{\phi-aL_\phi}{(1-a)L_\phi} & \text{for } aL_\phi<L_\phi \end{cases} \tag{3}$$

and periodicity is taken into account by $V_{\mathrm{rat}}(\phi)=V_{\mathrm{rat}}(\phi+L_\phi)$. The number of potential minima N_{min} determines the angular period $L_\phi=2\pi/N_{\mathrm{min}}$ and the asymmetry parameter a is defined as the ratio between the angular width of the short side of the sawtooth and the angular period L_ϕ. Finally, for a given trap radius R, the spatial period of the sawtooth potential is $L=RL_\phi=2\pi R/N_{\mathrm{min}}$.

In literature, several models for the time-dependence of the ratchet potential are known.[40] In this article, we use a fluctuating

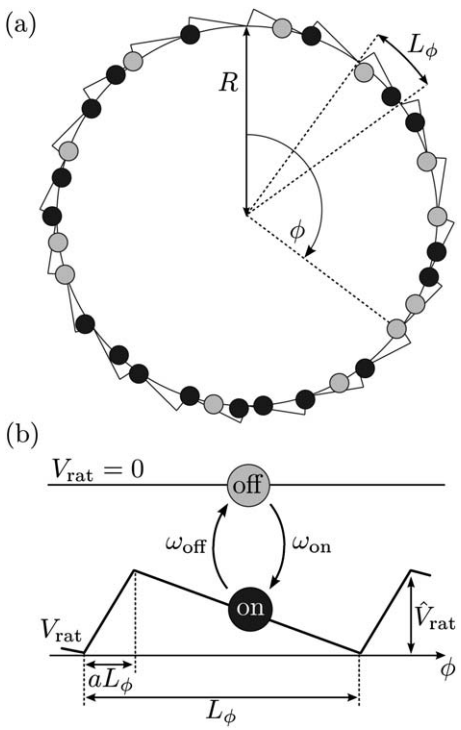

Fig. 1 (a) Toroidal trap with $N=30$ particles and radius $R=20\sigma$. A ratchet potential with $N_{\mathrm{min}}=20$ minima and asymmetry parameter $a=0.1$ is schematically shown. (b) The two states of the ratchet potential V_{rat}: the off-state with zero potential and the on-state with a sawtooth potential characterized by the angular period L_ϕ, the potential amplitude $\hat{V}_{\mathrm{rat}}$, and the asymmetry parameter a. The stochastic transition between both states is governed by the transition rates ω_{on} and ω_{off}.

 This journal is © The Royal Society of Chemistry 2011

Published on 24 December 2010 on http://pubs.rsc.org | doi:10.1039/C0SM01085E
Downloaded by TU Berlin - Universitaetsbibl on 23 March 2012

ratchet potential. In such a ratchet, the potential changes stochastically between two states: the on-state, in which the particle feels a force according to the ratchet potential V_{rat}, and the off-state, in which the particle diffuses freely along the trap. The transition between both states is governed by the rates ω_{on} and ω_{off}. We investigate two different scenarios for the stochastic transitions. In the first scenario, the ratchet state changes simultaneously for all particles and they are always in the same state. In the second scenario, each particle changes its state individually. As a consequence, particles in different states coexist in the trap. We further introduce the position-dependent transition rate $\hat{\omega}_{\mathrm{off}}(\phi)$ such that the rate is increased to $\omega_{\mathrm{off}}b$ in a narrow interval around each minimum, while it is decreased to ω_{off}/b anywhere else along the circle. The interval has the width of 1 deg and is centered around each minimum. This position dependence localizes the transitions from the on to the off-state in the vicinity of the potential minima. The parameter $b>1$ defines the strength of this localization. For $b = 1$, the transition rate does not depend on the particle position.

For all simulations, we set the potential amplitude to $\hat{V}_{\mathrm{rat}}/k_{\mathrm{B}}T = 100$ where $k_{\mathrm{B}}T$ is the thermal energy. As a consequence, the induced drift by the ratchet potential dominates the motion of particles in the on-state.

2.3. Hydrodynamic interactions

Colloidal particles are immersed in a fluid. As a consequence, forces acting on particles also influence all the other particles through induced flow fields. Due to the linearity of the Stokes equations, the translational velocities $\dot{\boldsymbol{r}}_i$ depend linearly on the external forces $\boldsymbol{f}_j$ acting on all particles. The velocity of particle i can be written as

$$\dot{\boldsymbol{r}}_i = \sum_{j=1}^{N} \boldsymbol{\mu}_{ij}(\boldsymbol{r}_1, \ldots, \boldsymbol{r}_N)\boldsymbol{f}_j. \tag{4}$$

The hydrodynamic coupling of the translating particles is described by 3×3 mobility tensors $\boldsymbol{\mu}_{ij}$. In general, these tensors are functions of the complete spatial configuration of all particles.[3] In this article, we neglect the rotational motion of the particles.

In our quasi-one-dimensional system, hydrodynamic interaction mainly has the following effects. Consider three particles in the toroidal trap, with the particle in the middle being driven by an external force along the channel. The two adjacent particles only feel the trap potential. Whereas the particle in the middle pushes the preceding particle forward by its drift motion, due to hydrodynamic interaction it can also pull the succeeding particle forward for a certain time.

2.4. Langevin equation

The total external force on particle i is given by the sum of the trap force, the repulsive forces, and the ratchet force which we derive from the potentials defined in eqn (1)–(3):

$$\boldsymbol{f}_i = \boldsymbol{f}_{\mathrm{trap},i} + \boldsymbol{f}_{\mathrm{rat},i} + \sum_j \boldsymbol{f}_{\mathrm{rep},ij}. \tag{5}$$

In the following, we combine the individual forces $\boldsymbol{f}_i$ and positions $\boldsymbol{r}_i$ of the particles to the $3N$-dimensional vectors $\mathbf{f} = (\boldsymbol{f}_1,\ldots,\boldsymbol{f}_N)$ and $\mathbf{r} = (\boldsymbol{r}_1,\ldots,\boldsymbol{r}_N)$, respectively. Then, the particle trajectories of the N particle system are governed by the Langevin equation

$$\mathbf{Z}(\mathbf{r})\dot{\mathbf{r}} = \mathbf{f}(\mathbf{r},t) + \tilde{\mathbf{f}}(t). \tag{6}$$

The stochastic force $\tilde{\mathbf{f}}(t)$ is unbiased $\langle\tilde{\mathbf{f}}(t)\rangle = 0$ and its auto-correlation function obeys the fluctuation-dissipation theorem

$$\langle\tilde{\mathbf{f}}(t) \otimes \tilde{\mathbf{f}}(t')\rangle = 2k_{\mathrm{B}}T\mathbf{Z}(\mathbf{r})\delta(t - t'), \tag{7}$$

where $\otimes$ means tensorial product. The $3N \times 3N$ friction matrix $\mathbf{Z}$ is related to the mobility matrix $\mathbf{M}$ and the diffusion matrix $\mathbf{D}$, respectively, by the generalized Einstein relation

$$\mathbf{Z}^{-1} = \mathbf{M} = \mathbf{D}/(k_{\mathrm{B}}T). \tag{8}$$

The mobility matrix consists of the mobility tensors defined in eqn (4) as follows

$$M = \begin{bmatrix} \boldsymbol{\mu}_{11} & \cdots & \boldsymbol{\mu}_{1N} \\ \vdots & & \vdots \\ \boldsymbol{\mu}_{N1} & \cdots & \boldsymbol{\mu}_{NN} \end{bmatrix} \tag{9}$$

Approximative expressions for the mobility tensors are given in the following section.

2.5. Simulation method

In order to numerically integrate the Langevin equation, we use the algorithm of Ermak and McCammon.[42] The change of the particle positions after one simulation step during time interval $\mathrm{d}t$ is given by

$$\mathrm{d}\mathbf{r} = \mathbf{M}\mathbf{f}\mathrm{d}t + \mathbf{A}\mathrm{d}\tilde{\mathbf{r}}, \tag{10}$$

where the Wiener increment $\mathrm{d}\tilde{\mathbf{r}}$ is defined by

$$\langle\mathrm{d}\tilde{\mathbf{r}}\rangle = \mathbf{0} \text{ and } \langle\mathrm{d}\tilde{\mathbf{r}} \otimes \mathrm{d}\tilde{\mathbf{r}}\rangle = \mathbf{1}\mathrm{d}t. \tag{11}$$

The $3N \times 3N$ amplitude matrix $\mathbf{A}$ obeys the equation

$$\mathbf{A}\mathbf{A}^{\mathrm{T}} = 2\mathbf{D}. \tag{12}$$

During the simulation $\mathbf{A}$ is determined by a Cholesky decomposition of $\mathbf{D}$ which is definitely positive. In this article, we use the Rotne-Prager approximation in order to calculate the mobility matrix $\mathbf{M}$ in eqn (9) for a configuration of spherical particles. The mobility tensors are given as

$$\begin{aligned} \boldsymbol{\mu}_{ii} &= \mu\mathbf{1} \\ \boldsymbol{\mu}_{ij} &= \mu\left[\frac{3}{4}\frac{\sigma}{r_{ij}}\left(\mathbf{1} + \hat{\boldsymbol{r}}_{ij} \otimes \hat{\boldsymbol{r}}_{ij}\right) + \frac{1}{2}\left(\frac{\sigma}{r_{ij}}\right)^3\left(\mathbf{1} - 3\hat{\boldsymbol{r}}_{ij} \otimes \hat{\boldsymbol{r}}_{ij}\right)\right], \end{aligned} \tag{13}$$

where $\hat{\boldsymbol{r}}_{ij}$ is the normalized distance vector between particle i and j.[3] The self mobility $\mu = 1/(6\pi\eta\sigma)$ of a spherical particle is related to the Stokes friction coefficient, where η is the viscosity of the fluid. The complete list of parameters for the performed simulations is given in Table 1.

In order to analyze the particle dynamics, we calculate the mean velocity and the velocity auto-correlation function from the simulated particle trajectories. Based on the angular positions

Table 1 List of simulation parameters and the corresponding time and velocity scales (diffusion time given for $a = 0.1$)

Particle radius σ	0.5	μm
Trap radius R	10	μm
Trap coefficient A	5×10^{-7}	Nm^{-1}
Repulsion coefficient B	7.5×10^{-19}	Nm
Temperature T	300	K
Viscosity η	10^{-3}	Pas
Potential amplitude $\hat{V}_{rat}$	4.1×10^{-19}	Nm
Number of minima N_{min}	20	
Simulation time step dt	$<6.6\times10^{-4}$	s
Drift velocity v_{drift}	15.5	$\mu m s^{-1}$
Drift time t_{drift}	0.18	s
Diffusion time t_{diff}	0.22	s

of the particles at the beginning $[\phi_i(0)]$ and the end $[\phi_i(T)]$ of the simulation, the mean velocity is given by

$$\langle v\rangle = \frac{R}{N}\sum_{i=1}^{N}\frac{\phi_i(T)-\phi_i(0)}{T}. \tag{14}$$

Here, $\phi_i(t)$ is a continuous angular trajectory. It grows beyond the angle 2π, so it is not reset each time the particle passes $\phi = 0$. For all simulations in this article the simulation time T was chosen such that at least 10^4 individual ratchet cycles occurred. The velocity auto-correlation function is defined as

$$c(\tau) = \frac{1}{N}\sum_{i=1}^{N}\frac{\langle \Delta v_i(t)\Delta v_i(t+\tau)\rangle}{\sqrt{\left\langle \Delta v_i(t)^2\right\rangle\left\langle \Delta v_i(t+\tau)^2\right\rangle}} \tag{15}$$

with

$$\Delta v_i(t) = v_i(t) - \langle v\rangle. \tag{16}$$

All simulations have been done on a cluster of recent 64-bit Intel Xeon® processors.

3. Results and discussion

For a brief review of the ratchet effect we first discuss the single particle system. It also serves as a reference for the multi-particle systems which we discuss for spatially constant and localized transition rates in Sections 3.2 and 3.3.

3.1. Ratchet dynamics of a single particle

In Brownian ratchets the interplay between deterministic drift caused by the asymmetric potential and unbiased diffusion leads to a rectification of Brownian motion. We consider a particle that has just changed to the off-state and assume a ratchet potential with asymmetry parameter $a < 1/2$.

In the off-state, the particle diffuses freely along the trap. We now derive the probability density function for the particle to be at a certain position when it changes back to the on-state. First, the probability density function for the particle to change to the on-state after time t has elapsed is given by

$$p_{on}(t) = \omega_{on}\exp(-\omega_{on}t). \tag{17}$$

Hence, the average time the particle spends in the off-state is

$$\langle t\rangle_{off} = \int_0^\infty p_{on}(t)t\mathrm{d}t = 1/\omega_{on}. \tag{18}$$

Second, the probability density function to find the particle displaced by $\Delta\phi$ from its initial position ϕ_0 after time t has elapsed is given by a Gaussian distribution

$$\mathcal{D}(\Delta\phi, t) = \frac{1}{\sqrt{4\pi D_\phi t}}\exp\left(-\frac{(\Delta\phi)^2}{4D_\phi t}\right), \tag{19}$$

where $D_\phi = D/R^2$ is the diffusion constant for angular diffusion along the circular trap. Eventually, the probability density to find the particle displaced by $\Delta\phi$ from its initial position ϕ_0 when it returns to the on-state is given by

$$\begin{aligned}\mathcal{P}(\Delta\phi) &= \int_0^\infty p_{on}(t)\mathcal{D}(\Delta\phi, t)\mathrm{d}t \\ &= \sqrt{\frac{\omega_{on}}{4D_\phi}}\exp\left(-\sqrt{\frac{\omega_{on}}{D_\phi}}|\Delta\phi|\right).\end{aligned} \tag{20}$$

This function is symmetric and gives zero mean displacement as expected from free diffusion. However, due to the asymmetry of the ratchet potential and a mean bias of the initial position ϕ_0 towards a local mimimum, the fraction of $\mathcal{P}(\Delta\phi)$ reaching into a neighboring spatial period is larger in clockwise direction. As a consequence, the particle will on average travel clockwise along the trap in absence of any net force in this direction. The resulting mean velocity $\langle v\rangle$ defined in eqn (14) is the main measure in this article. As a reference velocity, we introduce the velocity $v_{drift} = \mu\hat{V}_{rat}/[(1-a)L]$ of a single particle solely driven by the force $\hat{V}_{rat}/[(1-a)L]$ that is exerted by the longer slope of the ratchet potential. Further we rescale the transition rate ω_{on} by the inverse of the time $t_{diff} = (aL)^2/D$ a particle needs to diffuse an average distance $aL/2$. The transition rate ω_{off} rate is referred to the inverse of the drift time $t_{drift} = (1-a)L/v_{drift}$ a particle spends on the longer slope of the ratchet potential. The numeric values of t_{drift}, v_{drift} and t_{diff} are given in Table 1.

Fig. 2 (a) depicts simulation results for the rescaled mean velocity $\langle v\rangle/v_{drift}$ as a function of $\omega_{on}t_{diff}$ for several values of the asymmetry parameter a. As known from literature, more asymmetric ratchet potentials, *i.e.*, those with smaller values of a, lead to larger mean velocities.[40,41] The maximum mean velocity occurs for a transition rate $\omega_{on} \approx t_{diff}$ that gives the particle a significant chance to reach the next spatial period by diffusion and keeps the duration of the off-state short.

Fig. 2 (b) shows the simulation results for the rescaled mean velocity v/v_{drift} as a function of $\omega_{off}t_{drift}$ for several values of the localization parameter b. For a spatially constant transition rate ($b = 1$), the mean velocity has a maximum value for $\omega_{off}t_{drift} \approx 10$. This means that for maximizing the mean velocity, it is rather beneficial to change to the off-state before reaching the minimum of the potential than being trapped at the minimum. For localized transition rates with $b > 1$, the mean velocities significantly increase and the maximum velocity occurs for a wider range of values ω_{off}. For $b = 100$, the maximum velocity reaches its maximum value. For very large values of b this value is reached virtually independent of ω_{off}. The mean velocity increases since the performance of the ratchet is optimized by the localized transition rate $\hat{\omega}_{off}(\phi)$. On the one hand, the localization reduces the probability for a particle to change to the off-state before it

Published on 24 December 2010 on http://pubs.rsc.org | doi:10.1039/C0SM01085E
Downloaded by TU Berlin - Universitaetsbibl on 23 March 2012

 This journal is © The Royal Society of Chemistry 2011

Published on 24 December 2010 on http://pubs.rsc.org | doi:10.1039/C0SM01085E
Downloaded by TU Berlin - Universitaetsbibl on 23 March 2012

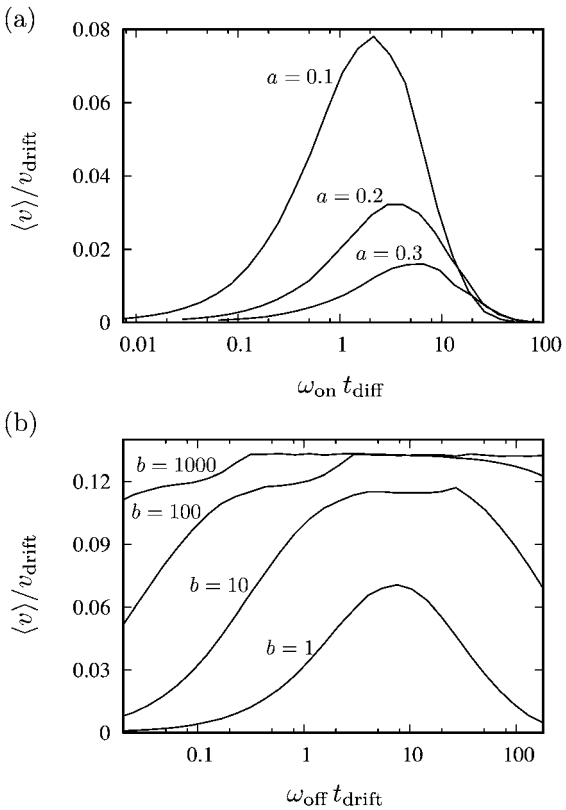

Fig. 2 Rescaled mean velocity $\langle v\rangle/v_{\rm drift}$ of a single particle, (a) as a function of $\omega_{\rm on}t_{\rm diff}$ for $a = 0.1$, 0.2 and 0.3 with $\omega_{\rm off}t_{\rm drift} = 3.6$ and $b = 1$. (b) as a function of $\omega_{\rm off}t_{\rm drift}$ for $b = 1$, 10, 100 and 1000 with $\omega_{\rm on}t_{\rm diff} = 4.5$ and $a = 0.1$.

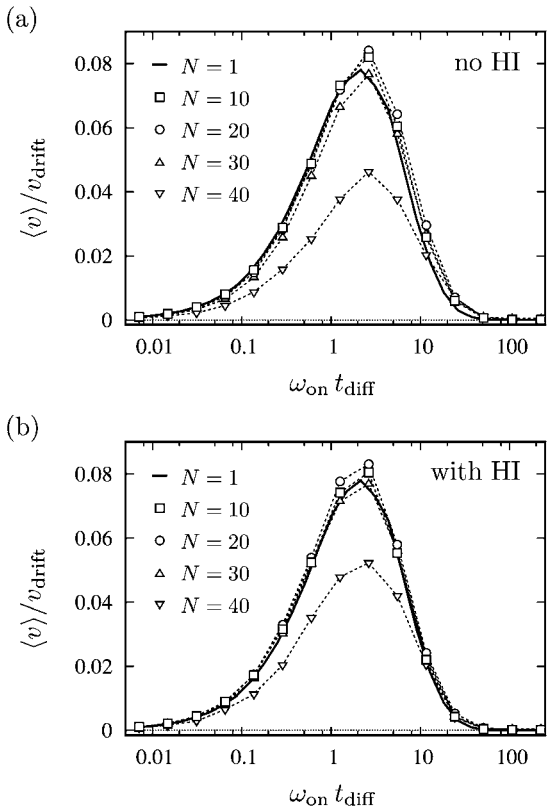

Fig. 3 Rescaled mean velocity $\langle v\rangle/v_{\rm drift}$ as a function of $\omega_{\rm on}t_{\rm diff}$ when particles change their ratchet states simultaneously. Simulation results for different particle numbers $N = 1$ (solid line), $N = 10$ (□), $N = 20$ (○), $N = 30$ (△), and $N = 40$ (▽) are plotted. Parameters are $\omega_{\rm off}t_{\rm drift} = 3.6$, $a = 0.1$, and $b = 1$. (a) without hydrodynamic interactions, (b) with hydrodynamic interactions.

reaches the potential minimum and hence increases the displacement during the on-state. On the other hand, the localization increases the probability to change to the off-state as soon as the potential minimum is reached. This keeps the time short during which the particle is trapped in the potential minimum.

For sufficiently large values of b, the particle will virtually always drift all the way towards the minimum and immediately change to the off-state. This optimized ratchet cycle gives the observed maximum value $\langle v\rangle/v_{\rm drift} \approx 0.13$ for the mean velocity in Fig. 2. As expected, this value is still smaller than the deterministic drift velocity $v_{\rm drift}$ even for highly optimized ratchet cycles. However, we will show in the subsequent sections that the ratio $\langle v\rangle/v_{\rm drift}$ increases significantly in multi-particle systems and even surpasses parity for localized transition rates.

3.2. Spatially constant transition rates

We now investigate multi-particle effects on the ratchet dynamics, in particular the effect of hydrodynamic interactions among the particles. We consider a ratchet potential with spatially constant transition rates and compare two scenarios where particles change the ratchet state either simultaneously or individually.

We first present the results when all particles always occupy the same state. Fig. 3 depicts the rescaled mean velocity $\langle v\rangle/v_{\rm drift}$ as a function of the rescaled transition rate $\omega_{\rm on}t_{\rm diff}$ for various particle numbers. With $\omega_{\rm off}t_{\rm drift} = 3.6$, the transition rate $\omega_{\rm off}$ has been chosen such that the mean velocity is close to the corresponding maximal value for any value of $\omega_{\rm on}$. Panel (a) shows the simulation results when hydrodynamic interactions are neglected (no HI) while in panel (b) hydrodynamic interactions are included (with HI). The maximum mean velocity is virtually unchanged for $N = 1$, 10, 20 and 30 particles. For $N = 40$ particles, the maximum mean velocity even drops by a factor of 0.6 compared to the single particle system. Hydrodynamic interactions hardly influence this behavior. Two effects due to the fixed sequential order of the particles in the toroidal trap reduce the mean velocity for large particle numbers. First, single-file diffusion occurs with sub-diffusional behavior of the mean square displacement $\Delta\phi^2 \sim t^{1/2}$, which is most pronounced when the particle number is large.[43] This slows down the spreading of the particle distribution function during the off-state and hence the mean velocity is reduced. Second, for large particle numbers the probability that two or more particles drift towards the same minimum increases. Since only one particle can occupy the position at the minimum, the drift of the other particles is hindered. This decreases the mean velocity not only by reducing the mean drift length but also by increasing the mean distance to the neighboring potential minimum.

The system's response for increasing particle numbers changes crucially when individual transitions of the particles between the ratchet states are allowed. For this scenario, Fig. 4 illustrates the rescaled mean velocity $\langle v\rangle/v_{\rm drift}$ as a function of the rescaled transition rate $\omega_{\rm on}t_{\rm diff}$ for various particle numbers by a factor of 2.2.

Published on 24 December 2010 on http://pubs.rsc.org | doi:10.1039/C0SM01085E
Downloaded by TU Berlin - Universitaetsbibl on 23 March 2012

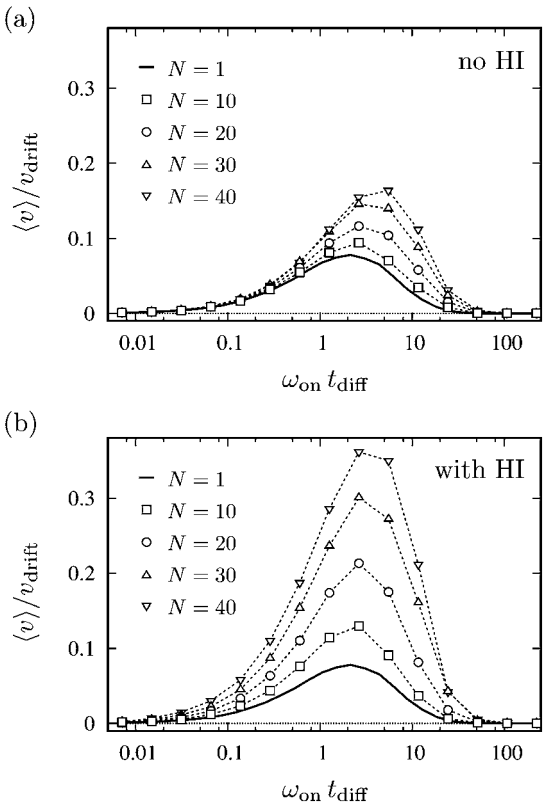

Fig. 4 Rescaled mean velocity $\langle v \rangle / v_{\mathrm{drift}}$ as a function of $\omega_{\mathrm{on}} t_{\mathrm{diff}}$ when particles change their ratchet states individually. Simulation results for different particle numbers $N = 1$ (solid line), $N = 10$ (□), $N = 20$ (○), $N = 30$ (△), and $N = 40$ (▽) are plotted. Parameters are $\omega_{\mathrm{off}} t_{\mathrm{drift}} = 3.6$, $a = 0.1$, and $b = 1$. (a) Without hydrodynamic interactions, (b) with hydrodynamic interactions.

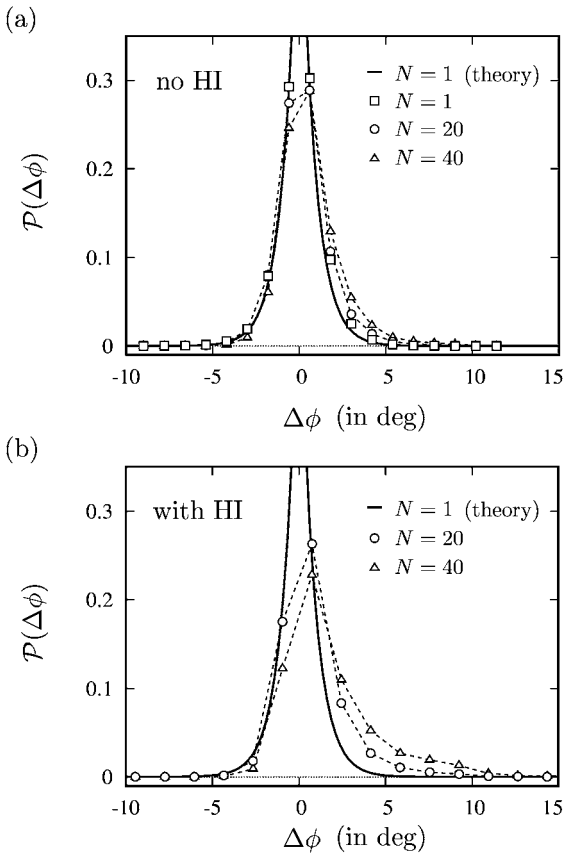

Fig. 5 The probability density function $\mathcal{P}(\Delta\phi)$ for a particle displacement $\Delta\phi$ at the moment when the particle changes to the on-state determined from the same simulation data as the graphs of Fig. 4. The curves belong to particle numbers $N = 1$ (□), $N = 20$ (○), and $N = 40$ (△), and the full line corresponds to the analytic expression of eqn (20) for a single particle. (a) Without hydrodynamic interactions, (b) with hydrodynamic interactions.

Panel (a) shows the simulation results when hydrodynamic interactions are neglected. Here, the maximum mean velocity increases with growing particle number. For $N = 40$ particles, $\langle v \rangle / v_{\mathrm{drift}}$ is larger than the single-particle value. Panel (b) shows the simulation results when hydrodynamic interactions are included. In contrast to the system with simultaneous transitions, hydrodynamic interactions now lead to a further significant increase of the mean velocity. For $N = 40$ particles, the mean velocity is larger by a factor of about 4.7 compared to the single-particle velocity. The following consideration provides a qualitative understanding of why the mean velocity increases when particles can switch individually between the on- and off-state. Particles in the on-state can push neighboring particles in the off-state due to repulsive interactions. Since the ratchet effect induces a mean drift clockwise along the longer potential slope, particles in the off-state are more likely pushed clockwise. When hydrodynamic interactions are included, drifting particles can also pull neighboring particles along which further enhances the mean velocity.

In order to analyze this mechanism quantitatively, we consider in Fig. 5 the probability density function $\mathcal{P}(\Delta\phi)$ for a particle to move a distance $\Delta\phi$ along the circle during off-time. The two graphs illustrate numerical results for $N = 1$, 20, and 40 particles and compare them to the theoretical prediction of eqn (20) for a single-particle system (full line). In panel (a) hydrodynamic interactions are not included. For $N = 1$, simulations give a symmetric and unbiased probability density $\mathcal{P}(\Delta\phi)$ in good agreement with the theoretical curve. For larger particle numbers the distribution is shifted towards positive values, *i.e.*, clockwise, whereby the induced bias increases with the number of particles. To be concrete, the mean value of the distribution is $\Delta\phi = 0.2$ deg for $N = 20$ particles and $\Delta\phi = 0.51$ deg for 40 particles. As a consequence, the probability for a particle to reach the neighboring potential minimum during the off-state and hence the mean velocity increases. Panel (b) shows the results when hydrodynamic interactions are included in the simulations. The induced bias of the probability distribution is further enhanced. For $N = 20$ particles, the mean value of the distribution is $\Delta\phi = 0.46$ deg for $N = 20$ particles and $\Delta\phi = 1.0$ deg for 40 particles. These mean values are now of the order of the length of the short slope of the ratchet potential ($aL_\phi = 1.8$ deg). It is noteworthy that the distribution is not symmetric any longer and the probability of particles being displaced by more than 5 deg is increased significantly. The long-range character of hydrodynamic interactions explains the enhanced bias of the distribution. A drifting particle not only pushes diffusing particles without being in direct contact but also pulls diffusing particles. Both mechanisms lead eventually to the observed increase of the mean velocities. In other words, the hydrodynamic coupling enhances the induced bias in diffusion.

This journal is © The Royal Society of Chemistry 2011

Published on 24 December 2010 on http://pubs.rsc.org | doi:10.1039/C0SM01085E
Downloaded by TU Berlin - Universitaetsbibl on 23 March 2012

We want to stress that this induced bias does not occur when all particles change their ratchet states simultaneously since then drifting particles cannot influence the diffusion of particles in the off-state. Individual transitions between the ratchet states are therefore a crucial requirement for the ratchet effect being enhanced by hydrodynamic coupling.

3.3. Localized transition rates

In this section we demonstrate that hydrodynamic interactions in combination with a localized transition rate $\hat{\omega}_{\mathrm{off}}(\phi)$ initiate the formation of transient particle clusters that move at high velocities. The underlying mechanism goes beyond the previously discussed induced bias in the diffusional off-state. Of course, the model is only realizable when the transitions between the on- and off-state occur individually for each particle. The transition rate from the on- to the off-state is $\omega_{\mathrm{off}}b$ when the particle reaches a potential minimum and ω_{off}/b otherwise.

Fig. 6 shows the velocity $\langle v\rangle$ in units of both v_{drift} and the one-particle value $\langle v\rangle_{N=1}$ as a function of the particle number N when hydrodynamic interactions are included as well as neglected. For the localization parameter $b = 100$, $\omega_{\mathrm{on}}t_{\mathrm{diff}} = 4.5$, and $\omega_{\mathrm{off}}t_{\mathrm{drift}} = 3.6$ the ratchet operates close to its maximum velocity. In both cases, the mean velocity increases with the particle number N. For 40 particles, the mean velocity is larger by a factor of 4.4 than the one-particle value when hydrodynamic interactions are neglected; in the presence of hydrodynamic interactions the factor assumes 10.3. It is remarkable that the mean velocity for $N \geq 30$ even surpasses the deterministic drift velocity v_{drift} when hydrodynamic interactions are included. In other words, the particles in the ratchet potential move faster than a single particle would travel that is driven by a constant force exerted by the longer slope of the ratchet potential. It is known that particles under the influence of a constant force in a toroidal trap move faster than a single particle due to reduced hydrodynamic drag.[36] In the following we discuss how clusters of particles in a ratchet potential can partially benefit from such a drag reduction and eventually surpass the velocity v_{drift}.

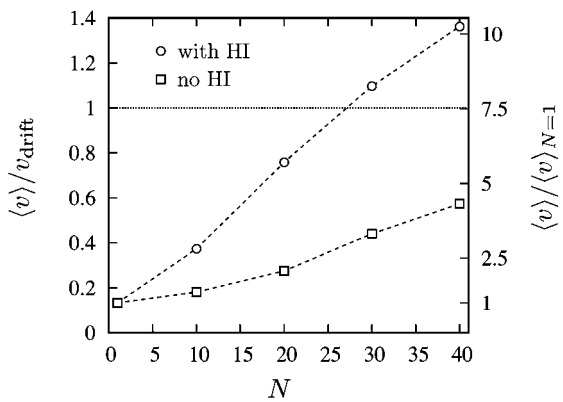

Fig. 6 Mean velocity $\langle v\rangle$ in units of v_{drift} (left ordinate) and $\langle v\rangle_{N=1}$ (right ordinate) as a function of particle number N. The parameters are $\omega_{\mathrm{on}}t_{\mathrm{diff}} = 4.5$, $\omega_{\mathrm{off}}t_{\mathrm{drift}} = 3.6$, $a = 0.1$, and $b = 100$. The symbols refer to simulation results including (○) and without (□) hydrodynamic interactions, respectively.

In order to reveal the underlying mechanism, we consider the example trajectories in Fig. 7 for a system with $N = 20$ particles. One set of trajectories is based on simulations including hydrodynamic interactions (HI); they have been neglected in the other set. The close-up of the trajectories in panel (b) (with HI) features strong variations in the particle density. In other words, clusters of particles with short distances occur spontaneously in the circular trap. These clusters travel with remarkably high velocities before they dissolve. The number of particles in such a transient cluster is not fixed. Rather, new particles join the cluster from the front and others are left behind at the rear end. When hydrodynamic interactions are neglected, as in panel (c), the spontaneous formation of transient clusters is not visible.

For a pair of particles, we explain in Fig. 8 how hydrodynamic interactions induce the formation of transient clusters which are then able to move with high velocities. We denote the particle in front with A and assume that it is located at the minimum of the ratchet potential where it has just switched into the off-state (grey). The second particle B is in the on-state (black) and drifts towards the minimum. It reaches the minimum without changing the state, due to the localization of $\hat{\omega}_{\mathrm{off}}$, and pushes particle A forward beyond the location of the potential barrier. Note that particle A needs to be in the off-state for this step. When particle B reaches the minimum, it immediately changes to the off-state. Ultimately, particle A assumes the on-state and drifts towards the next minimum. While doing so, it uses hydrodynamic interactions to pull particle B beyond the location of the potential

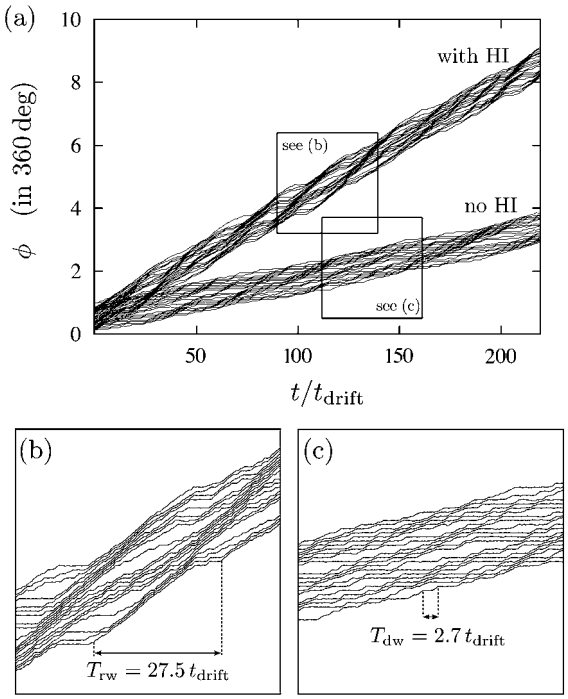

Fig. 7 (a) Particle trajectories $\phi(t)$ of $N = 20$ particles in the toroidal trap. The upper and lower set of trajectories refer to simulations where hydrodynamic interactions (HI) are included or neglected, respectively. The parameters are $a = 0.1$, $b = 100$, $\omega_{\mathrm{on}}t_{\mathrm{diff}} = 4.5$, and $\omega_{\mathrm{off}}t_{\mathrm{drift}} = 3.6$. The boxes indicate close-ups of the trajectories in panels (b) and (c). Examples of the run-walk cycle with duration T_{rw} and the drift-wait cycle with duration T_{dw} are indicated in (b) and (c), respectively.

Published on 24 December 2010 on http://pubs.rsc.org | doi:10.1039/C0SM01085E
Downloaded by TU Berlin - Universitaetsbibl on 23 March 2012

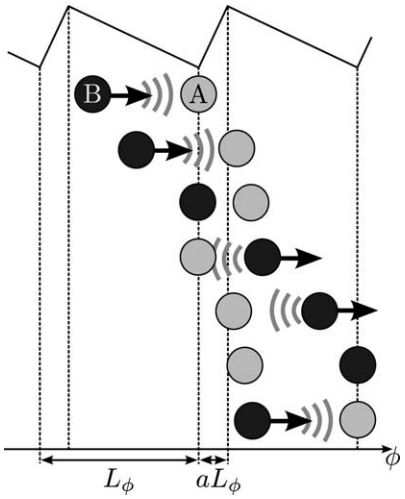

Fig. 8 Transient cluster formation of a pair of particles using hydrodynamic interactions. The front and rear particles are labeled A and B, respectively. The colors of the particles indicate the on-state (black) and the off-state (grey) in the ratchet cycle. The arrows show the drift direction in the ratchet potential and the grey arcs symbolize hydrodynamic interactions between the particles. The picture is explained in detail in the main text.

barrier. When particle A arrives at the next minimum and when particle B changes to the on-state, the initial configuration is reached; the cluster has moved one spatial period. Without hydrodynamic interactions this sequence is interrupted, as the leading particle A is not able to pull B while drifting into the next minimum and the cluster breaks up.

The motional pattern just described resembles the caterpillar-like motion that has been observed for colloidal particles in tilted sawtooth potentials.[37] The latter describes a fully deterministic pattern only disturbed by Brownian motion whereas the motion of the transient clusters has intrinsic stochastic elements: diffusion during the off-state and stochastic transition to the on-state. This stochastic character is the major difference to the caterpillar dynamics in ref. 37. The cluster dynamics has been demonstrated for a pair of particles. The presence of additional particles stabilizes the cluster since several pushing particles at the rear end and pulling particles at the front increase the probability that the cycle illustrated in Fig. 8 repeats itself.

Particles travelling in the observed clusters perform repetitive *drift-wait* cycles: they *drift* in the on-state to the next minimum, and subsequently *wait* until they are either pushed or pulled into the neighboring period by a front or rear particle, respectively. Note that the waiting period might last multiple ratchet cycles, as the particle might fail to reach the next period during off-time. In addition to this short-period drift-wait cycle, particles perform long-period *run-walk* cycles, where they *run* with high velocity as part of a cluster until they are left behind. Then, they *walk* as single particles with velocities lower than the overall mean velocity, until they join another cluster. When hydrodynamic interactions are neglected, the characteristic cluster formation does not occur but particles still perform drift-wait cycles. However, the waiting period now takes longer, since particles can reach the next period either by diffusion or by being pushed by a rear particle but not by hydrodynamic pulling. In Fig. 7 (b) and (c), examples for run-walk and drift-wait cycle are indicated, respectively. When hydrodynamic interactions are included, as in panel (b), the drift-wait cycles are too short to be properly visualized in the same figure.

In order to analyze the cycles just discussed quantitatively we use the velocity auto-correlation function $c(\tau)$ defined in eqn (15). If the deviation $\Delta v_i(t) = v_i(t) - \langle v \rangle$ of the particle velocity $v_i(t)$ from the mean value $\langle v \rangle$ is strictly periodic in time, the oscillations are reproduced by $c(\tau)$. However, due to the stochastic motion of the particles, $c(\tau)$ will tend to zero for large time differences τ. Fig. 9 depicts the velocity auto-correlation function $c(\tau)$ based on simulations with $N = 20$ particles. If hydrodynamic interactions are included, the correlation data indeed features two superimposed, damped oscillations with different periods. The period of the fast oscillation corresponds to the mean period of the drift-wait cycle $\langle T_{\mathrm{dw}} \rangle$, whereas the slow oscillation refers to the run-walk cycle with its mean period $\langle T_{\mathrm{rw}} \rangle$. From the correlation data, we find the values $\langle T_{\mathrm{rw}} \rangle = 28.6 t_{\mathrm{drift}}$ and $\langle T_{\mathrm{dw}} \rangle = 1.15 t_{\mathrm{drift}}$, respectively. Note that $\langle T_{\mathrm{rw}} \rangle$ is close to the value of one realization of the run-walk cycle illustrated in Fig. 7 (b). We also realize that $\langle T_{\mathrm{dw}} \rangle$ is smaller than the sum of drift time and mean off-time $t_{\mathrm{drift}} + \langle t \rangle_{\mathrm{off}} = 1.27 t_{\mathrm{drift}}$. Since $\langle t \rangle_{\mathrm{off}}$ is fixed this shows that the actual drift time $\langle T_{\mathrm{dw}} \rangle - \langle t \rangle_{\mathrm{off}} = 0.88 t_{\mathrm{drift}}$ is, on average, smaller than the single-particle drift time t_{drift} due to the reduced hydrodynamic drag in the cluster. In estimating the actual drift time, we already assumed that virtually all particles proceed to the neighboring potential minimum in one ratchet cycle while travelling in the cluster.

When hydrodynamic interactions are not included, the correlation data in Fig. 9 features only one oscillation that corresponds to the drift-wait cycle. Its mean period is $\langle T_{\mathrm{dw}} \rangle = 2.75 t_{\mathrm{drift}}$ which is significantly larger than the value reported in the previous paragraph when hydrodynamic interactions are taken into account. The main reason is that hydrodynamic pulling is absent which decreases the probability for a particle to proceed to the next period during off-time. Assuming that particles drift with the single-particle velocity, the average number of off-times per drift-wait cycle is $(\langle T_{\mathrm{dw}} \rangle - t_{\mathrm{drift}})/\langle t \rangle_{\mathrm{off}} = 6.5$. The particles

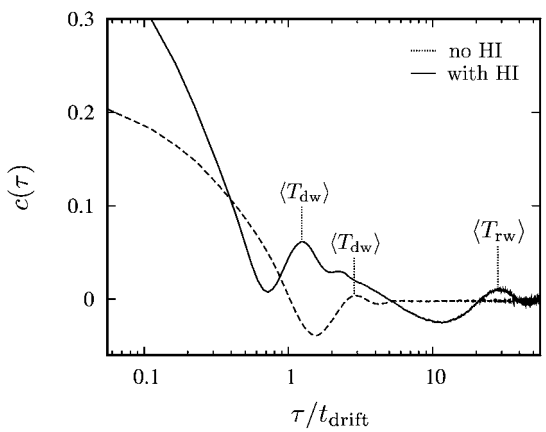

Fig. 9 Velocity auto-correlation functions $c(\tau)$ as a function of the rescaled time difference τ/t_{drift}. Solid and dotted lines refer to data where hydrodynamic interactions (HI) are included or neglected, respectively. The mean periods $\langle T_{\mathrm{dw}} \rangle$ and $\langle T_{\mathrm{rw}} \rangle$ of the drift-wait and run-walk cycles are indicated in units of t_{drift}.

 This journal is © The Royal Society of Chemistry 2011

need, on average, more than six ratchet cycles to reach the neighboring potential minimum. In this estimate, we have neglected the short on-times where the particles drift back to the minimum on the short slope since they have failed to pass the potential barrier during off-time.

4. Conclusions

In this article, we presented a thorough investigation of how hydrodynamic interactions among Brownian particles influence the performance of fluctuating thermal ratchets. In particular, we demonstrated that hydrodynamic interactions can significantly increase the particles' mean velocity. However, this is only possible when the particles change their ratchet states individually rather than simultaneously. Only then can drifting particles in the on-state act on neighboring particles in the off-state and add drift motion to their diffusional spreading. If in addition the transition rate from the on- to the off-state is localized at the minima of the ratchet potential, hydrodynamic interactions induce the formation of characteristic transient clusters. They travel with remarkably high velocities due to the reduction of the friction coefficient per particle in such a linear cluster.

Localized transition rates in ratchet systems are discussed in the context of modeling molecular motors.[44–46] On the other hand, recent theoretical work based on an extended ASEP model addressed the traffic of kinesin proteins along microtubulin complexes and showed that hydrodynamic interactions increase the mean velocity of the motor proteins and even cause cytoplasmic streaming.[38] Based on these works, Malgaretti and Pagonabarraga have also initiated work that studies the hydrodynamic coupling of molecular motors.[47] Similar to us, they also observe a strong increase in the mean velocity with the number of motors. Localized transition rates may also arise in molecular realizations of Brownian ratchets,[48,49] where individual molecules can be switched in to a potential-responsive state by random chemical events.

An early realization of a Brownian ratchet with colloidal particles uses circling optical tweezers, the intensity of which is modulated in order to create the sawtooth potential.[8] Realizing, in particular, a localized transition rate would require some feedback mechanism that monitors the particle position and switches off the sawtooth potential when a single particle reaches a minimum. A different feedback algorithm for particles whose states are switched collectively has already been demonstrated in the optical tweezer system.[11] It remains a challenge to experimentalists to construct the fluctuating ratchet where the particles change their states individually. In particular, when particles are close together this may cause difficulties.

Acknowledgements

We thank E. Frey and J.R.C. van der Maarel for helpful discussions and S. Klapp for bringing ref. 11 to our attention. A.G. thanks the research training group GRK1558 for financial support during his visits of TU Berlin.

References

1 J. Happel and H. Brenner, *Low Reynolds Number Hydrodynamics*, Noordhoff, Leyden, 1973.
2 S. Kim and S. J. Karrila, *Microhydrodynamics: Principles and Selected Applications*, Dover Publications, Mineola, NY, 2005.
3 J. K. G. Dhont, *An Introduction to Dynamics of Colloids*, Elsevier, Amsterdam, 1996.
4 P. N. Pusey, in *Liquids, Freezing, and Glass Transition, Proceedings of the Les Houches Summer School of Theoretical Physics 1989, Part II*, ed. J. P. Hansen, D. Levesque and J. Zinn-Justin, North-Holland, Amsterdam, 1991, pp. 763–942.
5 G. Nägele, *Phys. Rep.*, 1996, **272**, 215.
6 D. G. Grier, *Nature*, 2003, **424**, 810.
7 J. Rousselet, L. Salome, A. Ajdari and J. Prost, *Nature*, 1994, **370**, 446.
8 L. P. Faucheux, L. S. Bourdieu, P. D. Kaplan and A. J. Libchaber, *Phys. Rev. Lett.*, 1995, **74**, 1504.
9 S.-H. Lee, K. Ladavac, M. Polin and D. G. Grier, *Phys. Rev. Lett.*, 2005, **94**, 110601.
10 L. Gorre-Talini, S. Jeanjean and P. Silberzan, *Phys. Rev. E: Stat. Phys., Plasmas, Fluids, Relat. Interdiscip. Top.*, 1997, **56**, 2025.
11 B. J. Lopez, N. J. Kuwada, E. M. Craig, B. R. Long and H. Linke, *Phys. Rev. Lett.*, 2008, **101**, 220601.
12 A. Ajdari and J. Prost, *C. R. Acad. Sci., Ser. II*, 1992, **315**, 1635.
13 R. D. Astumian and M. Bier, *Phys. Rev. Lett.*, 1994, **72**, 1766.
14 J. Prost, J. F. Chauwin, L. Peliti and A. Ajdari, *Phys. Rev. Lett.*, 1994, **72**, 2652.
15 J. C. Crocker, *J. Chem. Phys.*, 1997, **106**, 2837.
16 J.-C. Meiners and S. R. Quake, *Phys. Rev. Lett.*, 1999, **82**, 2211.
17 M. Reichert and H. Stark, *Phys. Rev. E: Stat., Nonlinear, Soft Matter Phys.*, 2004, **69**, 031407.
18 S. Martin, M. Reichert, H. Stark and T. Gisler, *Phys. Rev. Lett.*, 2006, **97**, 248301.
19 R. E. Caflisch, C. Lim, J. H. C. Luke and A. S. Sangani, *Phys. Fluids*, 1988, **31**, 759.
20 I. K. Snook, K. M. Briggs and E. R. Smith, *Phys. A*, 1997, **240**, 547.
21 I. M. Janosi, T. Tel, D. E. Wolf and J. A. C. Gallas, *Phys. Rev. E: Stat. Phys., Plasmas, Fluids, Relat. Interdiscip. Top.*, 1997, **56**, 2858.
22 B. A. Grzybowski, H. Stone and G. M. Whitesides, *Nature*, 2000, **405**, 1033.
23 P. Lenz, J.-F. Joanny, F. Jülicher and J. Prost, *Phys. Rev. Lett.*, 2003, **91**, 108104.
24 N. Uchida and R. Golestanian, *Phys. Rev. Lett.*, 2010, **104**, 178103.
25 M. C. Lagomarsino, P. Jona and B. Bassetti, *Phys. Rev. E: Stat., Nonlinear, Soft Matter Phys.*, 2003, **68**, 021908.
26 A. Vilfan and F. Jülicher, *Phys. Rev. Lett.*, 2006, **96**, 058102.
27 T. Niedermayer, B. Eckhardt and P. Lenz, *Chaos*, 2008, **18**, 037128.
28 J. Kotar, M. Leoni, B. Bassetti, M. C. Lagomarsino and P. Cicuta, *Proc. Natl. Acad. Sci. U. S. A.*, 2010, **107**, 7669.
29 C. Wollin and H. Stark, unpublished results.
30 M. Kim and T. R. Powers, *Phys. Rev. E: Stat., Nonlinear, Soft Matter Phys.*, 2004, **69**, 061910.
31 M. Reichert and H. Stark, *Eur. Phys. J. E*, 2005, **17**, 493.
32 R. E. Goldstein, M. Polin and I. Tuval, *Phys. Rev. Lett.*, 2009, **103**, 168103.
33 T. Ishikawa and T. J. Pedley, *Phys. Rev. Lett.*, 2008, **100**, 088103.
34 C. M. Pooley, G. P. Alexander and J. M. Yeomans, *Phys. Rev. Lett.*, 2007, **99**, 228103.
35 R. Matas-Navarro and I. Pagonabarraga, *Eur. Phys. J. E*, 2010, **33**, 27.
36 M. Reichert and H. Stark, *J. Phys.: Condens. Matter*, 2004, **16**, 4085.
37 C. Lutz, M. Reichert, H. Stark and C. Bechinger, *Europhys. Lett.*, 2006, **74**, 719.
38 D. Houtman, I. Pagonabarraga, C. P. Lowe, A. Essling-Ozdoba, A. M. C. Emons and E. Eiser, *Europhys. Lett.*, 2007, **78**, 18001.
39 J. A. Fornes, *J. Colloid Interface Sci.*, 2010, **341**(2), 376.
40 P. Reimann, *Phys. Rep.*, 2002, **361**, 57.
41 A. Ajdari and J. Prost, *C. R. Acad. Sci., Ser. II*, 1992, **315**, 1635.
42 D. L. Ermak and J. A. McCammon, *J. Chem. Phys.*, 1979, **69**, 1352.
43 Q.-H. Wei, C. Bechinger and P. Leiderer, *Science*, 2000, **287**, 625.
44 F. Jülicher, A. Ajdari and J. Prost, *Rev. Mod. Phys.*, 1997, **69**, 1269.
45 R. Lipowsky and T. Harms, *Eur. Biophys. J.*, 2000, **29**, 542.
46 R. Lipowsky, *Phys. Rev. Lett.*, 2000, **85**, 4401.
47 P. Malgaretti and I. Pagonabarraga, *Running Faster, Running Together: Hydrodynamic Coupling of Molecular Motors*, International Soft Matter Conference 2010, Granada, Spain.
48 V. Balzani, A. Credi, F. M. Raymo and J. F. Stoddart, *Angew. Chem., Int. Ed.*, 2000, **39**, 3348.
49 V. Serreli, C.-F. Lee, E. R. Kay and D. A. Leigh, *Nature*, 2007, **445**, 523.

Published on 24 December 2010 on http://pubs.rsc.org | doi:10.1039/C0SM01085E
Downloaded by TU Berlin - Universitaetsbibl on 23 March 2012